Thin film of a topological insulator as a spin Hall insulator

R. S. Akzyanov
Dukhov Research Institute of Automatics, Moscow 127055, Russia;
Institute for Theoretical and Applied Electrodynamics, Russian Academy of Sciences, Moscow 125412, Russia;
and P.N. Lebedev Physical Institute of the Russian Academy of Sciences, Moscow 119991, Russia

(Received 24 January 2019; published 8 July 2019)

We study the spin conductivity of the surface states in a thin film of a topological insulator within Kubo formalism. Hybridization between the different sides of the film opens a gap at the Dirac point. We found that in the gapped region spin conductivity remains finite. In the gapless region near the band gap, spin conductivity is enhanced. These findings indicate that a thin film of a topological insulator is a promising material for spintronic applications.

DOI: 10.1103/PhysRevB.100.045403

I. INTRODUCTION

The spin Hall effect—generation of a transverse spin current by applied voltage—has been predicted in materials with spin-orbit scattering [1] and with strong spin-orbit interaction [2,3]. However, it has been shown that spin current in latter materials is small due to vertex corrections caused by point nonmagnetic disorder [4,5], which is consistent with the experimental data [6].

While spin current is dissipationless itself [2], the accompanying charge current is dissipative. An ideal material for the spintronics should have high spin conductivity along with low charge conductivity. In fact, a finite spin current can be produced in the insulators, where the charge current is absent due to the band gap. Such an effect is referred to as the quantum spin Hall effect (QSHE), and it is predicted in narrow gap semiconductors [7], graphene with enhanced spin-orbit interactions [8], and strained Rashba materials [9]. Also, QSHE is predicted in transition-metal dichalcogenides, but for experimentally relevant conditions spin Hall conductivity inside the gap does not occur [10].

Topological insulators have robust surface states that form a Dirac cone due to a topologically nontrivial band structure in the bulk [11]. Such materials have a potential in spintronics: record spin currents have been reported recently [12–16]. In a thin film finite hybridization between surface states opens a gap at the Dirac point [17,18]. We argue that finite spin conductivity exists in the gapped region of such a film.

In a previous paper, we studied the bulk and surface spin conductivity of thick topological insulators [19]. Also, spin conductivity in a thin film of a topological insulator was studied without taking into the account the intralayer scattering and vertex corrections in Ref. [20]. The case of the gapped surface states due to intralayer hybridization was missed. In this paper, we focus on the effects of finite hybridization between the surface states in a thin film of a topological insulator.

We calculate the spin conductivity of the surface states of a thin film of a topological insulator using Kubo formulas taking into account vertex corrections. We found that spin conductivity remains finite in the gapped region. Spin conductivity is enhanced near the gap in the metallic region. These finding can open the way for application of thin films of topological insulators in low dissipative spintronics.

II. MODEL

Low-energy surface states in the thin film of a topological insulator can be described by the Hamiltonian [17,18,21] ($\hbar = 1$)

$$\hat{H} = r\left(k_x^2 + k_y^2\right) + \mu + v_{Fk}(k_x\sigma_y - k_y\sigma_x)\tau_z + \Delta\tau_x,$$
$$v_{Fk} = v_F\left[1 + s\left(k_x^2 + k_y^2\right)\right], \tag{1}$$

where $\sigma = (\sigma_x, \sigma_y, \sigma_z)$ are the Pauli matrices acting in the spin space, $\tau = (\tau_x, \tau_y, \tau_z)$ are the Pauli matrices acting in the layer space, μ is the chemical potential, v_F is the Fermi velocity, $r = 1/(2m)$ is the inverse mass term, s characterizes the next order correction to the Fermi velocity, $k_x = k\cos\phi$ and $k_y = k\sin\phi$ are the in-plane momentum components, and Δ is the value of the gap at the Dirac point due to hybridization of the surface states belonging to different layers. The spectrum of the Hamiltonian (1) is doubly degenerate and is given by

$$E_\pm = \mu + rk^2 \pm \sqrt{v_F^2k^2(1+sk^2)^2 + \Delta^2}. \tag{2}$$

If we measure the energy in terms of v_F^2/r, then the chemical potential, the next-order correction to the Fermi velocity, and the gap are conveniently characterized by the dimensionless values $r\mu/v_F^2$, sv_F^2/r^2, and $r\Delta/v_F^2$, respectively.

The spectrum is shown at Fig. 1. This spectrum forms a Dirac cone when the inverse mass term is small, $sv_F^2/r^2 > 1/3$. In the opposite case, an additional Fermi surface with opposite helicity emerges for some values of chemical potential [19]. Note that the vanished inverse mass term $r = 0$ leads to vanished spin conductivity.

In general, the spin conductivity can be presented as a sum of three terms [22,23],

$$\sigma_{\alpha\beta}^{\gamma} = \sigma_{\alpha\beta}^{I\gamma} + \sigma_{\alpha\beta}^{II\gamma} + \sigma_{\alpha\beta}^{III\gamma}, \tag{3}$$

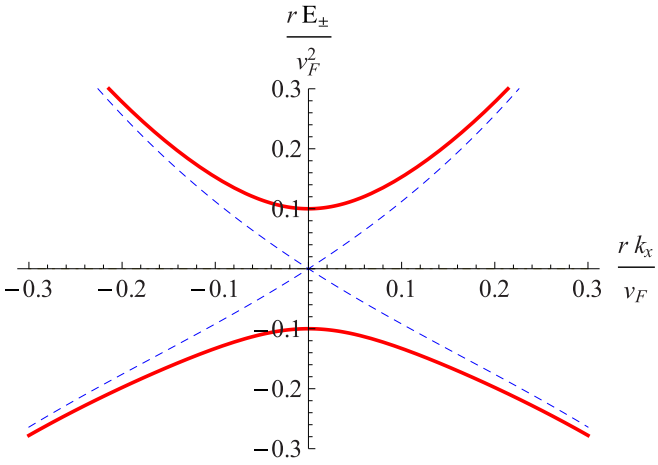

FIG. 1. Energy spectrum (2) for different values of the gap Δ for $sv_F^2/r^2 = 2$. Blue dashed line is the spectrum for zero gap $\Delta = 0$, and the red solid line is the spectrum for a finite gap $r\Delta/v_F^2 = 0.5$.

where the first two terms correspond to a contribution from the states at the Fermi level and the third one from the filled states. Here α and β denote the in-plane coordinates x and y, correspondingly, and γ denotes the spin projection.

At zero temperature the $\sigma_{\alpha\beta}^{I\gamma}$ and $\sigma_{\alpha\beta}^{II\gamma}$ contribution of states at the Fermi energy can be written as [4,22]

$$\sigma_{\alpha\beta}^{I\gamma} = \frac{e}{4\pi}\int \frac{d^2k}{(2\pi)^2}\mathrm{Tr}\left[j_\alpha^\gamma\, G^+ V_\beta\, G^-\right], \tag{4}$$

$$\sigma_{\alpha\beta}^{II\gamma} = -\frac{e}{8\pi}\int \frac{d^2k}{(2\pi)^2}\mathrm{Tr}\left[j_\alpha^\gamma\, G^+ V_\beta\, G^+ + j_\alpha^\gamma\, G^- V_\beta\, G^-\right]. \tag{5}$$

Here $j_\alpha^\gamma = \{\sigma_\gamma, v_\alpha\}/4$, $v_\alpha = \partial H/\partial k_\alpha$ is the velocity operator, $V_\alpha = v_\alpha + \delta v_\alpha$ is the velocity operator with vertex corrections δv_α, $\{,\}$ means the anticommutator, and $G^\pm$ are the retarded and advanced disorder averaged Green functions, which will be specified later.

The contribution to the spin conductivity from the filled states is

$$\sigma_{\alpha\beta}^{III\gamma} = \frac{e}{8\pi}\int \frac{d^2k}{(2\pi)^2}\int_{-\infty}^{\mu} f(E)dE \times \mathrm{Tr}\left[j_\alpha^\gamma\, G^+ v_\beta \frac{dG^+}{dE} - j_\alpha^\gamma \frac{dG^+}{dE} v_\beta\, G^+ + \text{c.c.}\right], \tag{6}$$

where $f(E)$ is the Fermi distribution function (that is, the Heaviside step for zero temperature), and c.c. means complex conjugate.

III. DISORDER AND VERTEX CORRECTIONS

We will describe disorder by a potential $V_{\text{imp}} = u_0\sum_i \delta(\mathbf{r} - \mathbf{R}_j)$, where $\delta(\mathbf{r})$ is the Dirac δ function, and $\mathbf{R}_j$ are the positions of the randomly distributed pointlike impurities with the local potential u_0 and concentration n_i. We assume that the disorder is Gaussian, that is, $\langle V_{\text{imp}}\rangle = 0$ and $\langle V_{\text{imp}}(\mathbf{r}_1)V_{\text{imp}}(\mathbf{r}_2)\rangle = n_i u_0^2\delta(\mathbf{r}_1 - \mathbf{r}_2)$. We introduce the disorder parameter as $\gamma_b = n_i u_0^2/(4v_F^2)$.

In the self-consistent Born approximation (SCBA), the impurity-averaged Green's functions can be calculated as $G^\pm = G_0^\pm + G_0^\pm\Sigma^\pm G^\pm$, where $G_0^\pm$ are bare retarded/advanced Green's functions of the Hamiltonian (1) and $\Sigma^\pm$ is the self-energy. Self-energy is defined as $\Sigma^\pm = \langle V_{\text{imp}} G^\pm V_{\text{imp}}\rangle$. In the case under consideration, we can calculate the self-energy $\Sigma^\pm = \Sigma' \mp i\Gamma$ using a Dyson equation $\Sigma^\pm = n_i u_0^2\sum_k G^\pm$. The self-energy has nontrivial structure in the side space τ. Along with the diagonal element $\Sigma_0\tau_0$ it has a nondiagonal one $\Sigma_x\tau_x$. Therefore, the expression for $G^\pm$ is similar to $G_0^\pm$, in which $\pm i0$ is replaced by $\pm i\Gamma_0$, μ by $\mu - \Sigma_0'$, and Δ by $\Delta - \Sigma_x' + i\Gamma_x$. The value Γ_0 describes the diagonal scattering rate while Γ_x describes the nondiagonal scattering rate.

We start with the case of large chemical potential $|\mu| \gg \Delta$. In this case we can neglect a small correction to the value of μ due to real part of the self-energy and put $\Sigma' = 0$. In this limit we suppose that scattering rates $\Gamma_0, \Gamma_x \to 0$ are small and we obtain that $\Gamma = \mathrm{Im}\Sigma^+ = n_i u_0^2\sum_k \mathrm{Im}G_0^+$.

Now we consider $r = s = 0$. In the metallic region $|\mu| > \Delta$ we get that the diagonal scattering rate is independent of chemical potential [24]:

$$\Gamma_0 = -\gamma_b|\mu|, \quad \Gamma_x = \gamma_b\Delta\mu/|\mu|. \tag{7}$$

The condition $\Gamma_0\Delta = -\Gamma_x\mu$ stands even for $|\mu| \gtrsim \Delta$. Near the band gap $|\mu| \simeq \Delta$ we calculate scattering rates self-consistently and found that the scattering rates are exponentially suppressed for a weak disorder $\Gamma_{0(x)} \propto e^{-2/(\pi\gamma_b)}$, which is expected for the Dirac system [25]. In the insulating region $|\mu| < \Delta$ condition, Eq. (7) fails and nondiagonal scattering is always smaller than diagonal scattering, $|\Gamma_0| > |\Gamma_x|$.

The impurity-averaged Green function can be calculated as $G^\pm = (1 + \Sigma G_0^\pm)^{-1}G_0^\pm$ or in the explicit form

$$G^\pm = \frac{\mu + rk^2 \pm i\Gamma_0 - v_{Fk}(k_x\sigma_y - k_y\sigma_x)\tau_z - (\Delta \pm i\Gamma_x)\tau_x}{(\mu + rk^2 \pm i\Gamma_0)^2 - \left[v_{Fk}^2k^2 + (\Delta \pm i\Gamma_x)^2\right]}. \tag{8}$$

In the SCBA, following the approach described in Ref. [26], we can derive an equation for the vertex-corrected velocity operator [27]:

$$V_\alpha(\mathbf{k}) = v_\alpha(\mathbf{k}) + \frac{n_i u_0^2}{(2\pi)^2}\int G^+(\mathbf{k})V_\alpha(\mathbf{k})G^-(\mathbf{k})d^2\mathbf{k}. \tag{9}$$

We found that hybridization Δ has little influence on the vertex corrections. For $r = s = 0$ we get a standard expression for the vertex-corrected velocity operator for the Dirac spectrum, $V_\alpha = 2v_\alpha$ [25,27].

Pointlike disorder renormalizes the k-independent part of the velocity operator. Thus, we write

$$V_x = v_x + \delta v\sigma_y\tau_z, \quad V_y = v_y - \delta v\sigma_x\tau_z, \tag{10}$$

where vertex corrections δv are calculated by the substitution of Eq. (10) into Eq. (9).

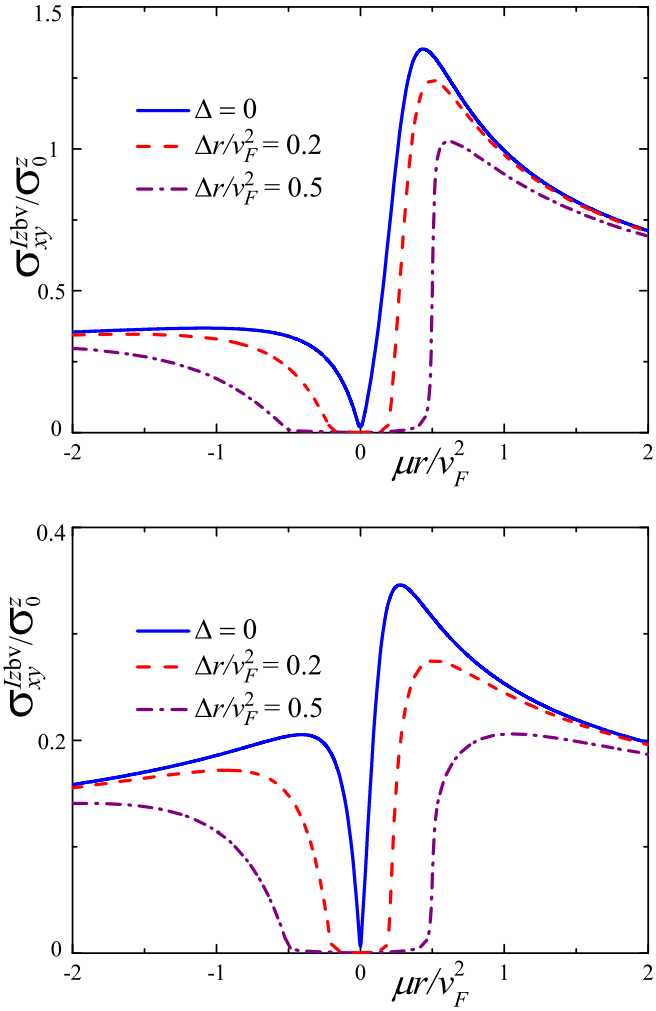

FIG. 2. Bare spin conductivity σ_{xybv}^{Iz} for $\gamma_b = 0.001$, $sv_F^2/r^2 = 1$ (upper panel), and $sv_F^2/r^2 = 5$ (lower panel). The blue line corresponds to $\Delta = 0$, the red dashed line to $r\Delta/v_F^2 = 0.2$, and the purple dot-dashed line to $r\Delta/v_F^2 = 0.5$.

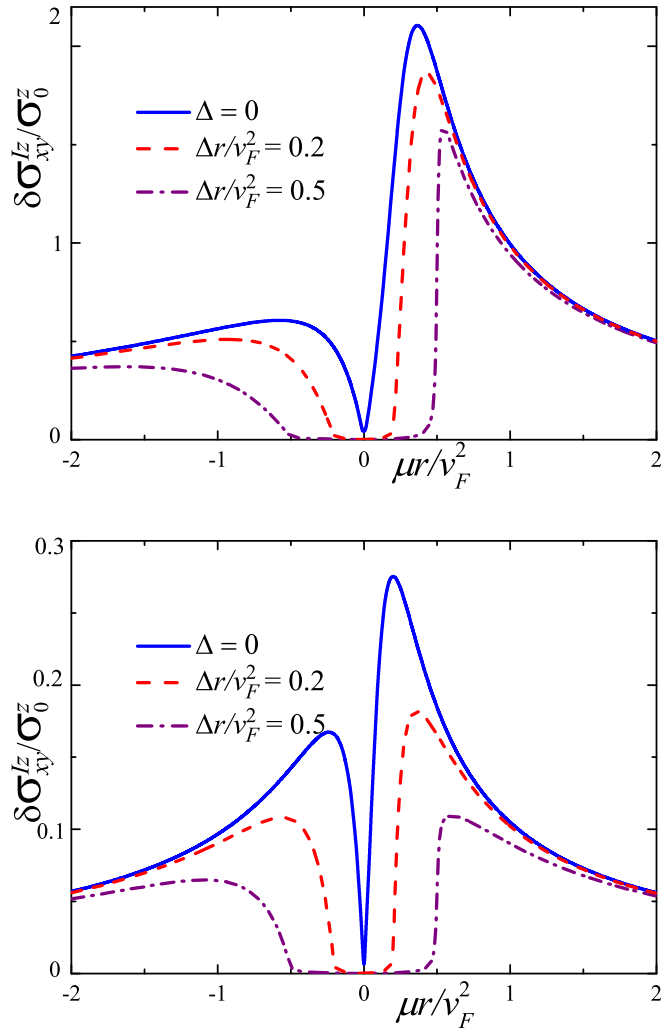

FIG. 3. Spin conductivity contribution from vertex corrections $\delta\sigma_{xy}^{Iz}$ for $\gamma_b = 0.001$, $sv_F^2/r^2 = 1$ (upper panel), and $sv_F^2/r^2 = 5$ (lower panel). The blue line corresponds to $\Delta = 0$, the red dashed line to $r\Delta/v_F^2 = 0.2$, and the purple dot-dashed line to $r\Delta/v_F^2 = 0.5$.

IV. SPIN CONDUCTIVITY FROM THE STATES AT THE FERMI SURFACE

Now we use the obtained results and Eqs. (4) and (5) to calculate the contribution to the spin conductivity due to the states at the Fermi surface. In this way, we obtained, first, that in the considered approach the term $\sigma_{\alpha\beta}^{II\gamma}$ vanishes exactly and we should compute the term $\sigma_{\alpha\beta}^{I\gamma}$ only.

The isotropic tensor component $\sigma_{xy}^{Iz} = -\sigma_{yx}^{Iz}$ is the only term that exists in the system. From Eq. (4), using the condition $\Gamma_0\Delta = \Gamma_x\mu$ we derive that

$$\begin{aligned}
\sigma_{xy}^{Iz} &= \sigma_{xy}^{Izbv} + \delta\sigma_{xy}^{Iz},\\
\sigma_{xy}^{Izbv} &= -\sigma_0^z \int k\,dk\,\frac{8r\Gamma_0 v_{Fk}^2 k^2}{\pi E_{g+}E_{g-}},\\
\delta\sigma_{xy}^{Iz} &= -\sigma_0^z \int k\,dk\,\frac{8r\Gamma_0 v_{Fk}\delta v k^2}{\pi E_{g+}E_{g-}},\\
E_{g\pm} &= (\mu + rk^2 \pm i\Gamma_0)^2 - v_{Fk}^2 k^2 - (\Delta \pm i\Gamma_x)^2. \quad (11)
\end{aligned}$$

Here σ_{xybv}^{Iz} is the spin conductivity without vertex corrections, and $\delta\sigma_{xy}^{Iz}$ is the spin conductivity contribution from the vertex corrections. We plot spin conductivity contributions as a function of the chemical potential for different values of the gap Δ and correction to the Fermi velocity s. Spin conductivity without vertex corrections is shown at Fig. 2. We can see that this contribution to the spin conductivity takes maximal value near the gap $\mu \sim \Delta$ and decreases with the increase of the gap. Contribution the spin conductivity from the vertex corrections is shown at Fig. 3. This contribution has a similar dependence on the value of chemical potential as the contribution without vertex corrections and is slightly smaller.

V. SPIN CONDUCTIVITY FROM THE FILLED STATES

We study Eq. (6) in a weak disorder limit. The isotropic component $\sigma_{xy}^{IIIz} = -\sigma_{yx}^{IIIz}$ is the only term that exists in the system. After energy integration using a constant damp approximation for Γ_0 we get that the contribution to the spin

conductivity from the filled states consists of two parts,

$$\sigma_{xy}^{IIIz} = \sigma_{xy0}^{IIIz} - \sigma_{xy}^{Izbv}, \tag{12}$$

where σ_{xy0}^{IIIz} is the spin conductivity in a clean limit, and σ_{xy}^{Izbv} is given by Eq. (11). Similar expressions have been obtain for the anomalous charge Hall conductivity for the Dirac Hamiltonian [28]. Spin conductivity from the filled states in a clean limit can be expressed as [3,29]

$$\sigma_{\alpha\beta 0}^{III\gamma} = e \sum_{\mathbf{k},n\neq n'} (f_{n\mathbf{k}} - f_{n'\mathbf{k}}) \frac{\mathrm{Im}\langle u_{n'\mathbf{k}}|j_\alpha^\gamma|u_{n\mathbf{k}}\rangle\langle u_{n\mathbf{k}}|v_\beta|u_{n'\mathbf{k}}\rangle}{(E_{n\mathbf{k}} - E_{n'\mathbf{k}})^2} \tag{13}$$

Here $E_{n\mathbf{k}}$ is the energy of an electron in the nth band with the momentum $\mathbf{k}$, $u_{n\mathbf{k}}$ is the corresponding Bloch vector, $\hat{H}u_{n\mathbf{k}} = E_{n\mathbf{k}}u_{n\mathbf{k}}$, $f_{n\mathbf{k}}$ is the Fermi distribution function corresponding to $E_{n\mathbf{k}}$ (which is the Heaviside step function in the considered case of zero temperature), Im is for the imaginary part, and $\langle ... \rangle$ is the scalar product. Using Eq. (13) we obtain

$$\sigma_{xy0}^{IIIz} = \sigma_0^z \int_0^\infty (\theta(E_+) - \theta(E_-))k\,dk \frac{2rk^2v_{Fk}^2}{\left(v_{Fk}^2 + \Delta^2\right)^{\frac{3}{2}}}, \tag{14}$$

where $\theta(x)$ is Heaviside step function and $\sigma_0^z = e/(8\pi)$ is the spin conductivity quanta. Finite disorder has a little impact on this term in the spin conductivity. The Heaviside step function $\theta(E_\pm)$ is replaced by the normalized arctangent function $2/\pi \arctan E_\pm/\Gamma_0$. This substitution leads to the insignificant blurring of the spin conductivity near the gap $\mu \simeq \pm\Delta$ for a small disorder. Spin conductivity in a clean limit σ_{xy0}^{IIIz} is shown in Fig. 4 for different values of the gap Δ and Fermi velocity correction s. Spin conductivity is a constant in the gapped region and decreases in the gapless region. Also, its particle-hole asymmetry is controlled by the parameter sv_F^2/r^2: asymmetry is smaller for larger values of the parameter. We can see that spin conductivity in a gapped region is comparable to the spin conductivity in a metallic region near the gap $\sigma_{xy0}^{IIIz}(\mu = 0, \Delta) \simeq \sigma_{xy0}^{IIIz}(\mu = \Delta, \Delta = 0)$, so at the Dirac point spin conductivity decreases with the increase of the gap Δ.

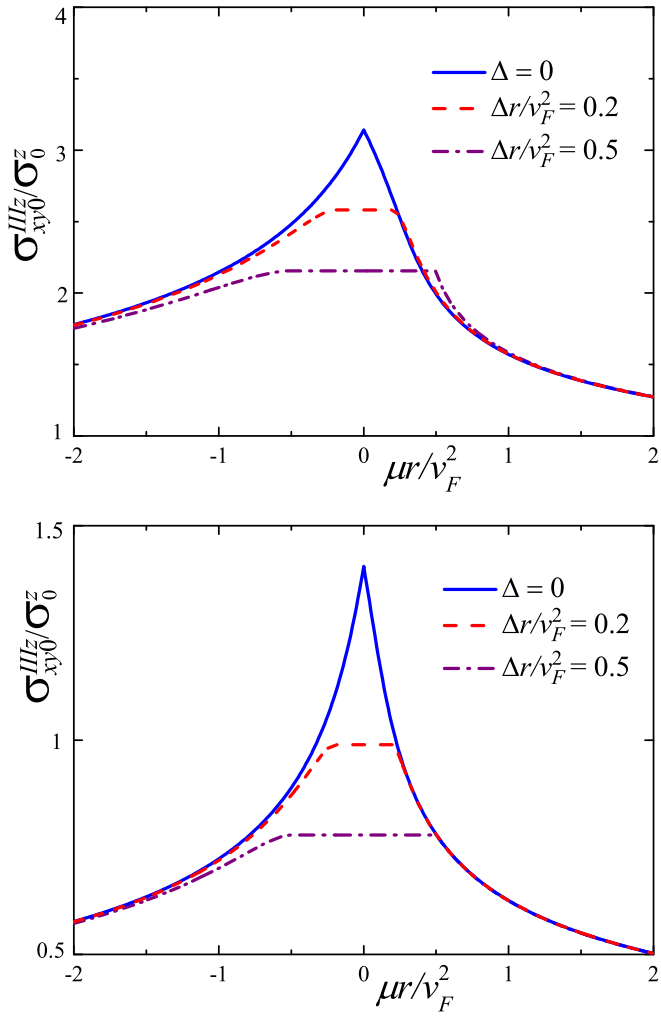

FIG. 4. Spin conductivity in a clean limit σ_{xy0}^{IIIz} as a function of chemical potential for $sv_F^2/r^2 = 1$ (upper panel) and for $sv_F^2/r^2 = 5$ (lower panel). The blue line corresponds to $\Delta = 0$, the red dashed line to $r\Delta/v_F^2 = 0.1$, the purple dot-dashed line to $r\Delta/v_F^2 = 0.5$, and the green line to $r\Delta/v_F^2 = 1$.

VI. ESTIMATES FOR THE EXPERIMENT

We can extract information on the disorder from the half-width of the quasiparticle peak in angle-resolved photoelectron spectroscopy (ARPES) from Ref. [30] and get $\gamma_b \sim 10^{-2}$. Scanning tunneling microscopy shows that there is approximately 1 defect per Å^2 for a clean surface [31]. If we suppose that the typical impurity potential is of the order of the chemical potential $\mu \sim 200$ meV (which is true for the vacation defects) and Fermi velocity for the surface states [32] $v_F \sim 3$ eV Å^{-1}, then we get an estimate for $\gamma_b \sim 10^{-3}$. The value of correction to the Fermi velocity s for the surface states is extracted from Ref. [33], and we get $sv_F^2/r^2 = 0.7$, where [34] $v_F^2/r = 1$ eV. Hybridization between the layers Δ depends strongly on the number of layers and reaches values of $\Delta = 0.2$ eV for two layers of Bi_2Te_3 [35].

We can see from Eqs. (11) and (12) that the term σ_{xy0}^{Iz} cancels out from σ_{xy}^{Iz} and σ_{xy}^{IIIz}. So, only contributions to the spin conductivity from the vertex corrections and spin conductivity in a clean limit remain. We plot total spin conductivity $\sigma_{xy}^z = \delta\sigma_{xy}^{Iz} + \sigma_{xy0}^{IIIz}$ as a function of chemical potential for the experimentally relevant parameters at Fig. 5. Spin conductivity remains finite inside the gap and is enhanced just outside of the gap. Also, it possesses considerable particle-hole asymmetry. Charge conductivity is calculated by [36], $\sigma_{xx} = \sigma_0/2\sum_{\mathbf{k}} V_x(G^+ - G^-)v_x(G^+ - G^-)$, where $\sigma_0 = e^2/\hbar$. Charge conductivity is suppressed inside the gap, and it has a weak dependence on the value of chemical potential away from the gap, as expected for the Dirac system [25].

VII. DISCUSSION

Spin conductivity exists in a gapped region of a topological insulator thin film, so this system is a spin Hall insulator. Spin conductivity is not changing inside the gap if we vary chemical potential. However, its value is not equal to the spin conductivity quanta, because the Hamiltonian does not commute with the z component of the spin $[H, \sigma_z] \neq 0$ [37], so spin is not conserved. In this way our system differs from

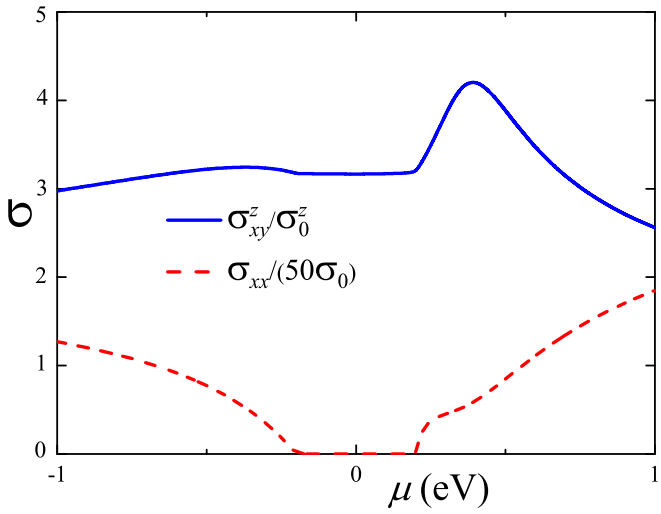

FIG. 5. Total spin conductivity σ^z_{xy} (blue line) and charge conductivity σ_{xx} (dashed red line) for the experimentally relevant data $\gamma_b = 0.01$, $sv_F^2/r^2 = 0.7$.

other spin Hall insulators [7–10]. In a similar way, charge quantum Hall conductivity is not quantized in superconductors, since charge is not conserved in such materials [38].

In the Kane-Mele–like models, where spin is conserved $[H, \sigma_z] = 0$, spin conductivity is generated by the spinful interaction between the Dirac cones $\sim\sigma_z$ [8,10]. In our model interaction between the Dirac cones is independent of the spin, and spin conductivity is generated by the intrinsic spin-orbit coupling, as expected for Rashba systems [3].

We suppose that both sides of the film are identical. In real samples asymmetry between different sides of the film can arise due to different doping and concentration of the defects. In a weak scattering limit, different scattering on the different sides of the film has almost no influence on the total spin conductivity if vertex corrections are neglected. However, significant asymmetry between the layers can have an effect on the vertex corrections.

Hybridization between layers, given by $\Delta\tau_x$, couples the electron (hole) from the Dirac cone of one layer to the hole (electron) of Dirac cone of another layer with the same spin. Such a bound state does not carry a charge but carries double spin and has spin-momentum locking of the parent electron. If we apply the electric field, then the flow of such bound states with zero charges will produce spin current without generation of an electric current.

The region inside the gap is of special interest. Scattering and dissipation are strongly suppressed due to an absence of the states at the Fermi energy. However, finite spin conductivity is present. Such a phase can be promising for low-dissipation spintronics applications.

Outside the gap spin conductivity is enhanced due to presence of the contribution of the states at the Fermi energy. This enhancement is significant only for thin films $\Delta \sim v_F^2/r$. If there are several layers then the gap is significantly suppressed in comparison with the mass parameter $\Delta \ll v_F^2/r \sim 1$ eV. For the four-layer film, the band gap reaches a value of $\Delta \sim 180$ meV and almost vanishes for thicker samples [35]. Thus, the effect of the enhancement of spin conductivity is significant only in samples of a few layers.

Experimentally, the dissipationless spin current can be measured by the spin-transfer torque effect [6,39]. If we apply voltage, then magnetization of the magnetic layer on the top of the topological insulator can be changed by the spin current without generation of the electrical current. Thus, the ratio of spin current to charge current—spin Hall angle—would be extremely large for such a system. However, the magnetic layer on the top should be an insulator to prevent shunting.

We do not consider the influence of the magnetic field on the spin conductivity. In real experiments on spin-transfer torque magnetic layers are used. Thus, the magnetization of the magnetic layer affects the value of the spin conductivity of the topological insulator. However, if magnetization is small (value of the Zeeman splitting is much smaller than chemical potential $|B| \ll |\mu|$), then its influence on the spin conductivity can be neglected.

Experiments on spin-transfer torque in a film of topological insulators with eight layers have been performed [12]. Good quality ultrathin films of topological insulators with a few layers are available [40,41]. The gap for the surface states is about 180 meV for the four-layer samples [42]. So, the measure of spin current in a thin-layer topological insulator inside and near the gap is as an experimentally achievable task.

To sum up, hybridization between the surface states in different layers of a thin film of a topological insulator opens a gap near the Dirac point. We found that finite spin conductivity exists in the gapped region. In a metallic region near the gap, spin conductivity is enhanced. These findings can be crucial towards the implementation of thin films of topological insulators in low-dissipation spintronics.

ACKNOWLEDGMENTS

We acknowledge support from the Russian Science Foundation Grant No. 17-12-01544, RFBR according to the research project No. 19-32-80014, and Foundation for the Advancement of Theoretical Physics and Mathematics BASIS.

[1] M. Dyakonov and V. Perel, Current-induced spin orientation of electrons in semiconductors, Phys. Lett. A **35**, 459 (1971).

[2] S. Murakami, N. Nagaosa, and S.-C. Zhang, Dissipationless quantum spin current at room temperature, Science **301**, 1348 (2003).

[3] J. Sinova, D. Culcer, Q. Niu, N. A. Sinitsyn, T. Jungwirth, and A. H. MacDonald, Universal Intrinsic Spin Hall Effect, Phys. Rev. Lett. **92**, 126603 (2004).

[4] J.-i. Inoue, G. E. W. Bauer, and L. W. Molenkamp, Suppression of the persistent spin Hall current by defect scattering, Phys. Rev. B **70**, 041303(R) (2004).

[5] R. Raimondi and P. Schwab, Spin-Hall effect in a disordered two-dimensional electron system, Phys. Rev. B **71**, 033311 (2005).

[6] J. Sinova, S. O. Valenzuela, J. Wunderlich, C. H. Back, and T. Jungwirth, Spin Hall effects, Rev. Mod. Phys. **87**, 1213 (2015).

[7] S. Murakami, N. Nagaosa, and S.-C. Zhang, Spin-Hall Insulator, Phys. Rev. Lett. **93**, 156804 (2004).

[8] C. L. Kane and E. J. Mele, Quantum Spin Hall Effect in Graphene, Phys. Rev. Lett. **95**, 226801 (2005).

[9] B. A. Bernevig and S.-C. Zhang, Quantum Spin Hall Effect, Phys. Rev. Lett. **96**, 106802 (2006).

[10] X. Li, F. Zhang, and Q. Niu, Unconventional Quantum Hall Effect and Tunable Spin Hall Effect in Dirac Materials: Application to an Isolated MoS_2 Trilayer, Phys. Rev. Lett. **110**, 066803 (2013).

[11] M. Z. Hasan and C. L. Kane, *Colloquium*: Topological insulators, Rev. Mod. Phys. **82**, 3045 (2010).

[12] A. R. Mellnik, J. S. Lee, A. Richardella, J. L. Grab, P. J. Mintun, M. H. Fischer, A. Vaezi, A. Manchon, E.-A. Kim, N. Samarth *et al.*, Spin-transfer torque generated by a topological insulator, Nature (London) **511**, 449 (2014).

[13] Y. Fan, P. Upadhyaya, X. Kou, M. Lang, S. Takei, Z. Wang, J. Tang, L. He, L.-T. Chang, M. Montazeri *et al.*, Magnetization switching through giant spin orbit torque in a magnetically doped topological insulator heterostructure, Nat. Mater. **13**, 699 (2014).

[14] Y. Wang, P. Deorani, K. Banerjee, N. Koirala, M. Brahlek, S. Oh, and H. Yang, Topological Surface States Originated Spin-Orbit Torques in Bi_2Se_3, Phys. Rev. Lett. **114**, 257202 (2015).

[15] Y. Fan, X. Kou, P. Upadhyaya, Q. Shao, L. Pan, M. Lang, X. Che, J. Tang, M. Montazeri, K. Murata *et al.*, Electric-field control of spin orbit torque in a magnetically doped topological insulator, Nat. Nano **11**, 352 (2016).

[16] N. H. D. Khang, Y. Ueda, and P. N. Hai, A conductive topological insulator with large spin Hall effect for ultralow power spin orbit torque switching, Nat. Mater. **17**, 808 (2018).

[17] H.-Z. Lu, W.-Y. Shan, W. Yao, Q. Niu, and S.-Q. Shen, Massive Dirac fermions and spin physics in an ultrathin film of topological insulator, Phys. Rev. B **81**, 115407 (2010).

[18] W.-Y. Shan, H.-Z. Lu, and S.-Q. Shen, Effective continuous model for surface states and thin films of three-dimensional topological insulators, New J. Phys. **12**, 043048 (2010).

[19] R. S. Akzyanov and A. L. Rakhmanov, Bulk and surface spin conductivity in topological insulators with hexagonal warping, Phys. Rev. B **99**, 045436 (2019).

[20] X. Peng, Y. Yang, R. R. Singh, S. Y. Savrasov, and D. Yu, Spin generation via bulk spin current in three-dimensional topological insulators, Nat. Commun. **7**, 10878 (2016).

[21] C.-X. Liu, X.-L. Qi, H. J. Zhang, X. Dai, Z. Fang, and S.-C. Zhang, Model Hamiltonian for topological insulators, Phys. Rev. B **82**, 045122 (2010).

[22] M.-F. Yang and M.-C. Chang, Středa-like formula in the spin Hall effect, Phys. Rev. B **73**, 073304 (2006).

[23] D. Kodderitzsch, K. Chadova, and H. Ebert, Linear response Kubo-Bastin formalism with application to the anomalous and spin Hall effects: A first-principles approach, Phys. Rev. B **92**, 184415 (2015).

[24] T. Kato, Y. Ishikawa, H. Itoh, and J. ichiro Inoue, Anomalous Hall effect in spin-polarized two-dimensional electron gases with Rashba spin orbit interaction, New J. Phys. **9**, 350 (2007).

[25] P. M. Ostrovsky, I. V. Gornyi, and A. D. Mirlin, Electron transport in disordered graphene, Phys. Rev. B **74**, 235443 (2006).

[26] N. Shon and T. Ando, Quantum transport in two-dimensional graphite system, J. Phys. Soc. Jpn. **67**, 2421 (1998).

[27] T. Chiba, S. Takahashi, and G. E. W. Bauer, Magnetic-proximity-induced magnetoresistance on topological insulators, Phys. Rev. B **95**, 094428 (2017).

[28] N. A. Sinitsyn, A. H. MacDonald, T. Jungwirth, V. K. Dugaev, and J. Sinova, Anomalous Hall effect in a two-dimensional Dirac band: The link between the Kubo-Streda formula and the semiclassical Boltzmann equation approach, Phys. Rev. B **75**, 045315 (2007).

[29] N. A. Sinitsyn, E. M. Hankiewicz, W. Teizer, and J. Sinova, Spin Hall and spin-diagonal conductivity in the presence of Rashba and Dresselhaus spin-orbit coupling, Phys. Rev. B **70**, 081312(R) (2004).

[30] C. Chen, Z. Xie, Y. Feng, H. Yi, A. Liang, S. He, D. Mou, J. He, Y. Peng, X. Liu *et al.*, Tunable Dirac fermion dynamics in topological insulators, Sci. Rep. **3**, 2411 (2013).

[31] P. Cheng, C. Song, T. Zhang, Y. Zhang, Y. Wang, J.-F. Jia, J. Wang, Y. Wang, B.-F. Zhu, X. Chen *et al.*, Landau Quantization of Topological Surface States in Bi_2Se_3, Phys. Rev. Lett. **105**, 076801 (2010).

[32] H. Zhang, C.-X. Liu, X.-L. Qi, X. Dai, Z. Fang, and S.-C. Zhang, Topological insulators in Bi_2Se_3, Bi_2Te_3 and Sb_2Te_3 with a single Dirac cone on the surface, Nat. Phys. **5**, 438 (2009).

[33] P. Rakyta, A. Palyi, and J. Cserti, Electronic standing waves on the surface of the topological insulator Bi_2Te_3, Phys. Rev. B **86**, 085456 (2012).

[34] M. Nomura, S. Souma, A. Takayama, T. Sato, T. Takahashi, K. Eto, K. Segawa, and Y. Ando, Relationship between Fermi surface warping and out-of-plane spin polarization in topological insulators: A view from spin- and angle-resolved photoemission, Phys. Rev. B **89**, 045134 (2014).

[35] T. Forster, P. Kruger, and M. Rohlfing, *GW* calculations for Bi_2Te_3 and Sb_2Te_3 thin films: Electronic and topological properties, Phys. Rev. B **93**, 205442 (2016).

[36] I. Proskurin, M. Ogata, and Y. Suzumura, Longitudinal conductivity of massless fermions with tilted Dirac cone in magnetic field, Phys. Rev. B **91**, 195413 (2015).

[37] O. F. Dayi and E. Yunt, Relation between the spin Hall conductivity and the spin Chern number for Dirac-like systems, Int. J. Geom. Methods Mod. Phys. **13**, 1550136 (2015).

[38] G. Bednik, A. A. Zyuzin, and A. A. Burkov, Anomalous Hall effect in Weyl superconductors, New J. Phys. **18**, 085002 (2016).

[39] D. Ralph and M. Stiles, Spin transfer torques, J. Magn. Magn. Mater. **320**, 1190 (2008).

[40] G. Zhang, H. Qin, J. Teng, J. Guo, Q. Guo, X. Dai, Z. Fang, and K. Wu, Quintuple-layer epitaxy of thin films of topological insulator Bi_2Se_3, Appl. Phys. Lett. **95**, 053114 (2009).

[41] D. Kim, P. Syers, N. P. Butch, J. Paglione, and M. S. Fuhrer, Coherent topological transport on the surface of Bi_2Se_3, Nat. Commun. **4**, 2040 (2013).

[42] M. Lang, L. He, X. Kou, P. Upadhyaya, Y. Fan, H. Chu, Y. Jiang, J. H. Bardarson, W. Jiang, E. S. Choi *et al.*, Competing weak localization and weak antilocalization in ultrathin topological insulators, Nano Lett. **13**, 48 (2013).